energies

MDPI

Article

An Experimental Investigation on the Performance of a Water Storage Tank with Sodium Acetate Trihydrate

Jie Huang [1], Fei Xu [2], Zilong Wang [1,*] and Hua Zhang [1]

[1] Institute of Refrigeration and cryogenic Engineering, School of Energy and Power Engineering, University of Shanghai for Science and Technology, Shanghai 200093, China
[2] Technical Center for Mechanical and Electrical Product Inspection and Testing of Shanghai Customs District, Shanghai 200135, China
* Correspondence: wzl@usst.edu.cn

Abstract: Phase change material (PCM) water tanks have a major influence on the efficiency improvement of solar energy systems. This article discusses the effects of PCM under various inlets in a tank based on related research. So as to research the performance of the water storage tank, this paper built a set of water tank experimental systems using sodium acetate trihydrate. The thermal characteristics of two different water tanks were analyzed at 2, 6 and 10 L/min when the inlet temperature was 20 °C and the initial high temperature was 80 °C. The test results indicate that adding PCMs helps to provide an extra 1.4% of stored heat, prolong the hot water outlet time, and has a better thermal stratification, compared with ordinary water tanks. However, PCMs do not give off heat quickly at high flow rates. Besides the exergy efficiency (EE) gradually decreasing, the MIX number first decreases and then increases; the fill efficiency (FE) has the opposite trend with the flow increasing. FE has a max of 0.905 at 6 L/min.

Keywords: water storage tank; PCM; thermal stratification

check for updates

Citation: Huang, J.; Xu, F.; Wang, Z.; Zhang, H. An Experimental Investigation on the Performance of a Water Storage Tank with Sodium Acetate Trihydrate. *Energies* **2023**, *16*, 777. https://doi.org/10.3390/en16020777

Academic Editor: Asif Ali Tahir

Received: 6 November 2022
Revised: 25 December 2022
Accepted: 28 December 2022
Published: 9 January 2023

1. Introduction

Phase change technology plays a significant role in heating storage which aims to improve the efficiency of renewable energy systems. Increasing heat storage capacity has great significance for most systems. Thermal stratification of phase change storage tanks plays an important role in improving the heat storage properties of solar heating systems and water tanks. In recent year, heat storage technology has become one of hot issue of concern for global experts and scholars [1–3]. Several studies have been performed on enhancing heat storage energy and the other properties of water tanks [4–6]. Hua et al. [7] designed a set of PCM water storage tank systems with uniform orifice plates. As the outlet flow was 3.3 L/min, the composite water tank with 60 PCM balls produced 10 L more hot water above 333.15 °C than the pure water tank. Zhou et al. [8] tested the response characteristics of hot water charging and the discharging of the water tank with PCMs on the side wall. It was shown that, compared with the traditional structure water tank, this new water tank could decrease the outlet temperature from 67 °C to 40 °C and extend this procedure for 10 h. Based on experiments, Brumleve et al. [9] demonstrated the possibility of using natural thermocline to allow high- and low-temperature water discrimination in the water tank. Frazzica et al. [10] studied variation laws of PCMs on domestic water heating systems which contained hydrated salt mixtures. Research has shown that when adding 1.3 dm^3 PCMs into the storage tank, it could store 10% more energy. Ramana et al. [11] concluded that increasing the weight of the PCMs led to effectively improving stratification in the tank. In this case, the efficiency of solar collectors and heat storage systems had a substantial increase. Moreover, another improvement method is also proposed that lowers the mass flow. Through experimental verification and simulation software analysis, among them, the heat storage capacity of spherical capsules has become a hot research topic recently. The dynamic properties of a latent heat thermal energy storage system packaged by spherical capsules, which were encapsulated by sodium nitrate from both experimental and numerical simulation aspects, were analyzed under high temperature conditions by Bellan [12]. The Stefan number is a significant dimensionless number to discuss the influence of sensible heat. Moreover, when the coefficient of the thermal conductivity of the package reduces, the influence of the package thickness increases. Kumar et al. [13] investigated the variation mechanism of a water tank containing a PCM while the heat storage process happened. In comparison to the water tank without PCMs, the heat retaining capacity of the PCM water tank increased first and then decreased along with the inlet temperature increasing. While the inlet temperature was 70 °C, the maximum temperature increased to about 1.3 %. Panchabikesan et al. [14] created new experimental models. A cylindrical tank is filled with spherical encapsulated PCMs and a nozzle is installed before water flows into the tank. For the proposed hybrid cooling system, the heat storage duration is reduced by 28.7% as the velocity of the inlet was 2 m/s, while it is reduced by 34.8% with the inlet velocity of 1.5 m/s. Koca et al. [15] applied $CaCl_2 \cdot H_2O$ in a solar collector, analyzed the PCMs that had a positive influence on the heat storage from energy and exergy. The net energy efficiency arrived at 45% and the minimum average exergy efficiency was 2.2% and the capacity was superior to the common water tank. An certainamount of work has been devoted to modularizing phase change heat storage, namely PCMs which were are designed in various shapes. Some results have been tested and have verified that PCMs' modularization would significantly increase the energy density of the water tank by two to three times [16,17]. Furthermore, different types of materials have different thermal storage effects. Paraffin as a common organic heat storage material possess a good heat storage capacity. In Navarro's research, by laying PCMs balls composed of a paraffin mixture and polyethylene on the top of the tank, the heat release time for the tank was evidently prolonged. To reduce PCMs' leakage in experiment, carrying out at least 25 thermal cycles was necessary [18]. Because of the smaller occupied area of PCM heat exchangers, Prieto et al. [19] experimentally verified the energy characteristics of three micro-cogeneration systems which used PCM heat exchangers and were suitable for 450 square meters of office space. In this paper, by analyzing the dynamic characteristics, palmitic acid and RT60 paraffin presented their heat thermal storage effect, such that palmitic acid had more energy storage per unit volume, and could meet the heat needs of the system with fewer storage units. In addition, Najafian et al. [20] added PCMs to a standard domestic hot water tank. The experiments proved the hot water outlet time, the quantity and diameter of the balls encapsulated in the PCM, and the vertical location of the phase change material balls had a close correlation. Furthermore, latent heat storage was more beneficial to store heat than sensible thermal storage. The additional PCMs in the hot water system could greatly alleviate the power consumption during peak periods. Other parameters, such as inlet flow, the aspect ratio of the PCM water tank, and the inlet water temperature, also have a certain influence on the thermal stratification characteristics [21,22]. Aspect ratio as an important parameter was studied in Afshan's research. Putting PCM balls in an experimental tank whose aspect ratio is 1:1 could help to stratify temperature zones. Moreover, as the value of the aspect ratio increases, the stratification number increases as well as the energy density [23]. An increased temperature leads to more pronounced thermal stratification. Phase change materials as a medium could transfer a great deal of latent heat during the phase transition process. Therefore, the PCMs had a high energy density and remained in a narrow temperature fluctuation during the process of phase transformation. Hot water was available for longer periods of time as the PCMs were used in water tanks [24–27]. Apart from experiments, numerical simulation is also a significant research technique to study temperature distribution in PCM water tanks. Bony and Citherlet [16] set up a numerical model to study a water tank which was easy to change and deform the heat storage modules and the different kinds of materials. When theoretically analyzing the heat storage effect of materials, the enthalpy approach using paper considered hysteresis and supercooling. Berkel [28] found in his research that the temperature in the tank undergoes a brief thermocline process during water injection. Through changing the inlet and outlet structure, there is a suitable structure that can make thermoclinic performance best. Likewise, other scholars have discussed different tank structures in numerical simulation methods [29–31].

Regarding the above literature review, the features of thermal stratification in PCM water tanks should be investigated deeply. Thus, the objectives of this paper are to investigate the temperature and energy change process of each layer in a water tank whose volume is 60 L and which include phase change balls, especially in releasing heat. The change principle of inlet flow on the thermal stratification characteristics is compared; moreover, the thermal stratification characteristics are evaluated by dimensionless parameters such as mixing number, filling efficiency (FE), and exergy efficiency (EE).

2. Experimental System and Uncertainty Analysis

2.1. Apparatus Introduction

The discharging process inside the high-temperature tank was displayed on an energy storage heating system. The main components in the experimental apparatus were the water delivery piping, a cylindrical PCM hot water tank, a water recovery system, and an outer circulation water system, as shown in Figures 1 and 2.

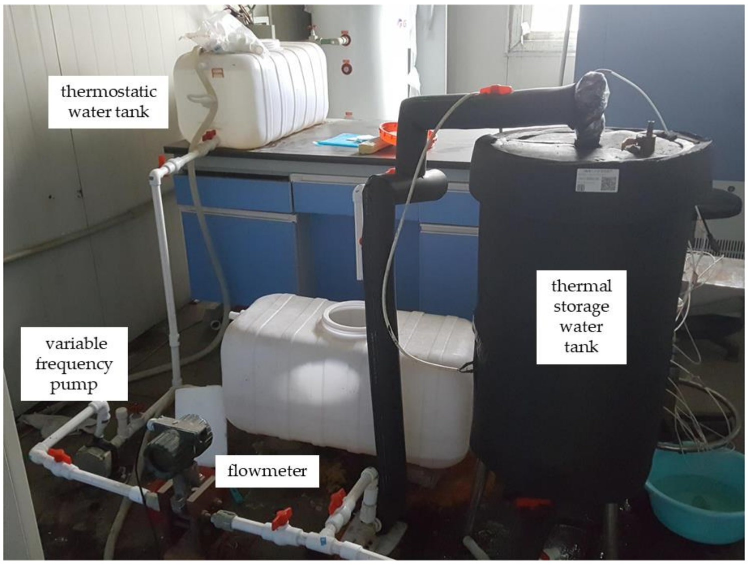

Figure 1. Example of the experimental device.

Before the test began, in the first place, municipal water, which is driven by the variable frequency water pump, fills the constant temperature tank (120 L) and the test tank and maintains the initial temperature (20 °C) through an intrinsic circulation water system. Secondly, the electric heating rod whose rated power is 1.5 KW can play the role of solar energy and heat the cold water to 80 °C. After the experiment started, municipal water flows into the water tank. Then, it passes through the flow equalizer which is composed of large, medium, and small cavities to the equalize water. The municipal water enters the radial holes of the small cavity and then flows into the medium cavity. What is more, the cold water changes the flow direction and outflows from bottom holes of the large cavity. Finally, the liquid level rises steadily. The cold water exchanges the heat with the PCM balls and the initial hot flow. The water pump is turned on and the temperature in the tank is controlled at 80 ± 0.3 °C, with the high temperature flow being exported from the top of the tank. The workflow conditions become 2, 6, and 10 L/min. When the inlet temperature is approximately equal to the outlet temperature, the system is shut down and the data collection is stopped.

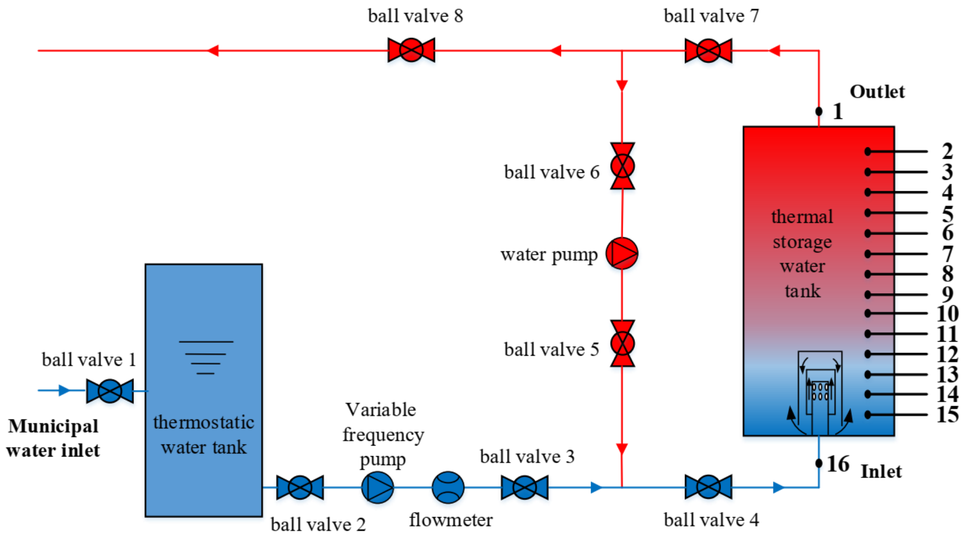

Figure 2. Experimental schematic diagram of the hot water tank with PCMs.

For the purpose of minimizing heat leakage from the tank body and the surrounding water pipes, heat insulation cotton (thermal conductivity of 0.024 W/(m·K)) is applied for heat insulation protection and 43 phase change heat storage balls (each volume is 3×10^{-3} m^3) are placed on the shelf. The device installation and geometric dimensions inside the tank are shown in Figure 3b.

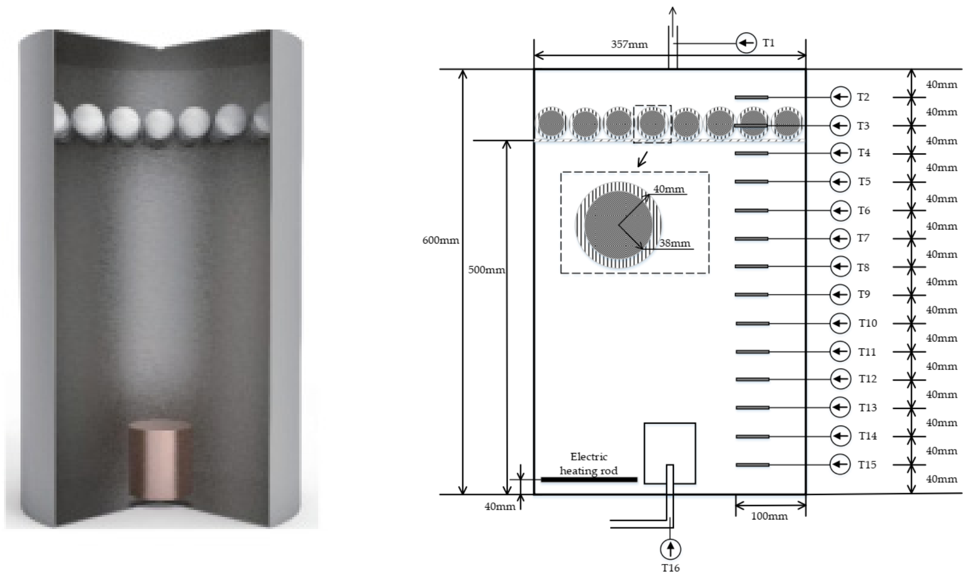

(**a**) Three-dimensional schematic diagram (**b**) Two-dimensional geometric dimension drawing

Figure 3. The structure of the hot water storage tank with PCMs.

Sodium acetate trihydrate (SAT) as one potential storage chemical compound absorbed a lot of heat energy in the experiment. The measurement results with differential scanning calorimeter (DSC) showed that pure SAT would occur as supercooling and in phase separation which has an effect on the energy transfer efficiency of the phase change material when arriving at the phase transition temperature range of 58~62 °C. For improving the shortcomings of pure SAT, in this experiment, disodium hydrogen phosphate dodecahydrate reduced supercooling by accelerating the crystallization rate, gelatin could inhibit phase separation, and the mixture was stirred and mixed by a constant temperature heating bath. The thermophysical properties of the PCMs that were measured by the DCS and the thermal constant analyzer are displayed in Table 1. Since the sodium acetate trihydrate mixture is placed in the water tank for a long time, the oxidation–reduction reaction occurs. PCMs need to be encapsulated in a 40 mm-diameter PVC sphere with a thermal resistance of 0.005 ($m^2 \cdot K$)/W and a 1 mm wall thickness. as shown in Figure 4.

Table 1. Thermophysical properties of the phase change heat storage sphere.

Thermophysical Property	Unite	Value
Latent heat	$kJ \cdot kg^{-1}$	250
Specific heat capacity	$kJ \cdot (kg\ K)^{-1}$	2.719
Thermal conductivity	$W \cdot (m \cdot K)^{-1}$	0.8
Density	$kg \cdot m^{-3}$	1520
Phase transition temperature	°C	58/62
Latent heat	$kJ \cdot kg^{-1}$	250

Figure 4. Phase change heat storage sphere.

The experimental measurement equipment used in this experiment are as follows: a vortex flowmeter (model Krohne OPTIFLUX 5300, measurement accuracy of ±0.15%, flow display range is 1 L/min–12 L/min), a data collector (model Agilent 34970A), and PT100 platinum resistance (measurement accuracy of ±0.5 °C). The whole system includes 16 PT100 platinum resistance. Among them, there are 14 platinum resistors in the water tank, labeled respectively as 2–15. In addition, each platinum resistor represents a temperature measuring point position, namely measuring points 2–15. Measuring point 1 is arranged on the water tank inlet pipe and measuring point 16 is arranged on the water tank outlet pipe, so their temperatures could be measured respectively. The geometric dimensions of the fourteen platinum resistors in the hot water tank which are in a uniform vertical arrangement are shown in Figure 3b. Agilent 34970A as a temperature acquisition instrument connects the computer and the 16 platinum resistance thermometers. At the same time, Agilent 34970A receives the voltage signal of the flowmeter for collection. The computer data acquisition software can acquire the temperature data, and the acquisition interval is 5 s.

For the purpose of verifying the profit by adding the PCM of the heat storage capacity in the tank, there is a need to run a set of tests with no PCMs in the experimental rig. In this experiment, only the hot water storage tank needs to be filled up, and there is no need to place PCMs.

2.2. Uncertainty Analysis

When measuring the temperature and flow in the experiments, due to the inaccuracy of the measurement tools, there are errors in the test results. Therefore, the standard error is specified as the criterion for judging the experimental uncertainty. The uncertainty (expressed as σ) in the tests is given by:

$$\sigma = \sqrt{\frac{\sum \left(X_i - \overline{X}\right)^2}{n}} \quad (1)$$

where X_i is the i-th experiment value and $\overline{X}$ is the arithmetic mean of the experiment values.

3. Thermal Properties

3.1. Dimensionless Time

According to the experimental design, there is a large difference between each inlet flow. This means that there are different water volumes at different inlet flows at the same time. To facilitate comparing the stratification features in the tank under different flows, dimensionless time τ can be used as a complex index measure of the water storage time which can be computed by comparing the water inlet time (t) to complete a replacement of the whole tank water under the current flow time (T):

$$\tau = \frac{t}{T} \tag{2}$$

3.2. Water Tank Capacity

The amount of energy that the water tank can store is an intuitive standard which can reflect the thermal performance of the PCM. The initial temperature of the water is set to 20 °C, and then it is heated to 80 °C. The water tank's accumulated energy is calculated in ordinary working conditions and working conditions containing PCMs.

While calculating the cumulative energy in the ordinary tank, its expression is as follows:

$$Q_{\mathrm{w}} = C_{\mathrm{p}} \cdot \rho_{\mathrm{w}} \cdot V_{\mathrm{T}} \cdot (T_{\mathrm{hot}} - T_{\mathrm{cold}}) \tag{3}$$

When calculating the cumulative energy in the PCMs tank, its expression is as follows:

$$Q_{\mathrm{PCM}} = C_{\mathrm{P}} \cdot \rho_{\mathrm{w}} \cdot (V_{\mathrm{T}} - V_{\mathrm{P}}) \cdot (T_{\mathrm{hot}} - T_{\mathrm{cold}}) + V_{\mathrm{p}} \cdot \rho_{\mathrm{PCM}} \cdot [C_{\mathrm{pl}} \cdot (T_{\mathrm{hot}} - T_{\mathrm{l}}) + L + C_{\mathrm{ps}} \cdot (T_{\mathrm{s}} - T_{\mathrm{cold}})] \tag{4}$$

Compared with Equation (3), the cumulative energy contains energy that is absorbed by water from 20 °C to 80 °C. On the other hand, Equation (4) also involves the sensible heat and latent heat of the PCM balls.

3.3. Fill Efficiency

In previous studies in the authors' laboratory, it was found that the inlet water temperature was not only an influencing factor for the stratified properties of water tanks, but also for the the initial water temperature, the inlet flow. Accordingly, for the purpose of intuitively expressing the stratified characteristics of the water tank, FE is proposed as a characteristic parameter [32].

The water tank begins to pass through a certain time t from the moment of entering the water, and the energy of the effluent is

$$Q_{\mathrm{exp}} = \int_0^t \dot{m} \cdot \rho_{\mathrm{w}} \cdot C_{\mathrm{P}} \cdot (T_{\mathrm{exp}} - T_{\mathrm{in}})dt \tag{5}$$

Similar to Equation (5), a perfectly stratified tank stockpiles energy, which could be expressed by Equation (6).

$$Q_{\mathrm{str}} = \int_0^t \dot{m} \cdot \rho_{\mathrm{w}} \cdot C_{\mathrm{P}} \cdot (T_{\mathrm{hot}} - T_{\mathrm{in}})dt \tag{6}$$

The FE is:

$$\overline{\xi} = \frac{Q_{\mathrm{exp}}}{Q_{\mathrm{str}}} \tag{7}$$

where Q_{exp} means energy stored in the experimental water tank (J) and Q_{str} means the energy stored in the ideal stratified water tank (J).

As a thermal stratification index, FE indicates the degree of thermal distribution. When the FE value is 0, it represents water that has been fully mixed in the experimental tank; when the filling efficiency is 1, it represents the perfect stratified water tank. That means with the value of FE increasing, the more available energy the tank can store and the greater the thermal efficiency.

3.4. MIX

Based on the weighted calculation of vertical location, Davidson et al. [33] proposed the MIX number to measure the mutual immersion degree between high- and low-temperature water quantitatively.

In Equations (8)–(11), the heat loss coefficient through thermocline is not included. During calculations, the experimental tank momentum (M_{exp}) is determined in the following two theoretical cases: the first case is perfect stratification, represented by M_{str}, and the second case is full mixing represented by M_{m}.

$$MIX = \frac{M_{\mathrm{str}} - M_{\mathrm{exp}}}{M_{\mathrm{str}} - M_{\mathrm{m}}} \tag{8}$$

$$E_i = \rho \cdot V_i \cdot C_{\mathrm{P}} \cdot T_i \tag{9}$$

$$M_{\mathrm{exp}} = \sum_{i=1}^{\mathrm{n}} y_i \cdot E_i \tag{10}$$

$$E_{\mathrm{exp}} = \sum_{i=1}^{\mathrm{n}} E_i \tag{11}$$

where

$$E_{\mathrm{stratified}} = E_{\mathrm{exp}} \tag{12}$$

$$E_{\mathrm{stratified}} = V_{\mathrm{hot}} \cdot \rho \cdot C_{\mathrm{P}} \cdot T_{\mathrm{hot}} + V_{\mathrm{cold}} \cdot \rho \cdot C_{\mathrm{P}} \cdot T_{\mathrm{cold}} \tag{13}$$

$$V_{\mathrm{T}} = V_{\mathrm{hot}} + V_{\mathrm{cold}} \tag{14}$$

The volume of hot and cold water can be determined according to Equations (12)–(14). T_{hot} and T_{cold} could be tested in the experiement.

$$V_{\mathrm{h}} = \pi \cdot \frac{D^2}{4} \cdot (H - y_{\mathrm{s}}) \tag{15}$$

According to V_{h} and V_{c} and the thermocline location, the perfect stratified tank momentum is:

$$M_{\mathrm{s}} = \sum_{i=1}^{\mathrm{n}} E_{\mathrm{s},i} \cdot y_i \tag{16}$$

The variation range of MIX is 0–1, wherein MIX = 0 represents perfect stratification of the tank, and MIX = 1 represents the tank fully mixing.

3.5. Exergy Efficiency

Njoku et al. [34] analyzed numerical, experimental, and theoretical results during charging process in a water tank. They thought that exergy efficiency could be a standardized to estimate the useful energy, so that a computing method could be proposed. The equations are represented as:

$$\xi = E - \sum_{i=1}^{\mathrm{n}} C_{\mathrm{p}} \cdot m_i \cdot T_{\mathrm{in}} \cdot \ln\left(\frac{T_i}{T_{\mathrm{in}}}\right) \tag{17}$$

$$E = \sum_{i=1}^{\mathrm{n}} C_{\mathrm{p}} \cdot m_i \cdot (T_i - T_{\mathrm{in}}) \tag{18}$$

The EE could be written in the form:

$$\xi^* = \frac{\xi_e}{\xi_s} \tag{19}$$

4. Experimental Result Analysis

4.1. Temperature

Figure 5 shows the variations in the temperature measuring points 1, 3, 5, 8, and 15 with dimensionless time in the PCM water tank under several inlet flow conditions. For comparison, the measured data of the water tank without a PCM are also shown.

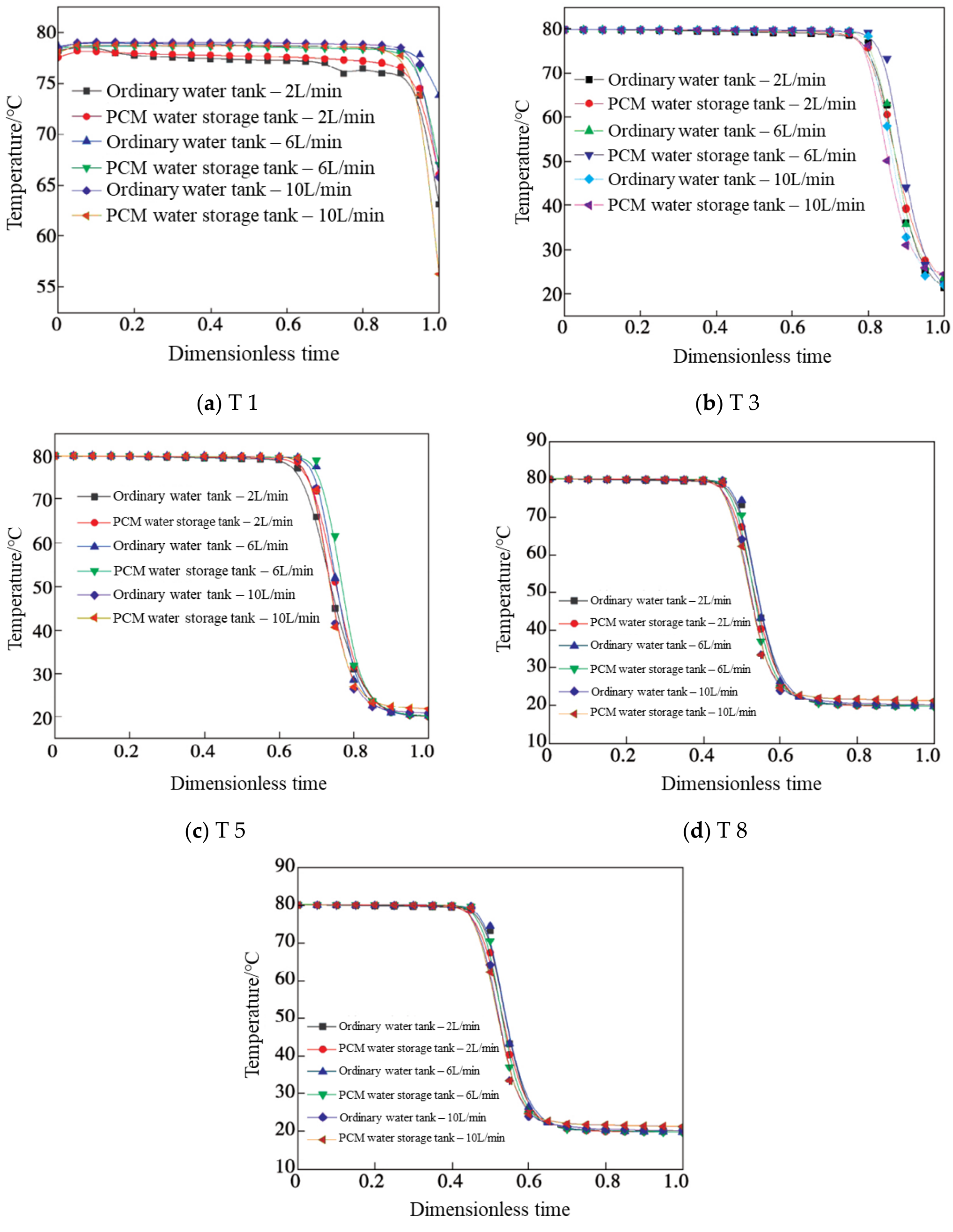

(**a**) T 1 (**b**) T 3 (**c**) T 5 (**d**) T 8 (**e**) T 15

Figure 5. Temperature variations in the hot water tank.

Figure 5 illustrates that the temperature of the five measuring points of the water tank will experience a sharp temperature drop after maintaining the initial temperature for some hours, then gradually approach the inlet temperature. The inflection point indicates that municipal water starts to blend with 80 °C hot water in the experimental tank. Figure 5a–e shows that municipal water evenly mixed upward with the original water layer-by-layer in the tank under the effect of a flow equalizer. The replacement process ends until the high temperature water in the whole tank is also cooled. The variation trend of each layer's temperature with dimensionless time in the PCMs tank is basically the same as that in the ordinary water tank. Point three tests the temperature layer where the PCM balls are located. As the inlet flow arrives at 6 L/min, the temperature inflection points in the ordinary operating condition and the operating condition that had SAT are at the dimensionless times of 0.8 and 0.85, respectively. During this process, phase change material balls can provide their own latent heat to display a reheat effect on the temperature stratification, which can delay the temperature inflection point. While the inlet flow increases up to 10 L/min, the measure to increase the SAT balls does not play the expected reheating effect, but the temperature decreases rapidly. This is because high flow strengthens the disturbance between hot and cold water, and the original thermal stratification is destroyed. Apart from this, a large quantity of municipal water rapidly absorbs lots of energy evidently, thus reducing the volume of hot water and the thickness of the thermocline is further increased.

Points 8 and 15 are far away from the heat storage layer and are below the PCMs, so that the PCMs have an extremely weak reheat effect. For point 15, dimensionless time can only be delayed by 0.002 as the inlet flow equals 2 L/min. At this time, the region affected by the inlet water flow is much greater than the impact of the PCMs, and the temperature curve is basically coincident.

Figure 6 depicts the effect of phase change materials on outlet temperature, except for the analysis on the measuring points in the tanks from Figure 5. Because measuring point 1 reflects the water discharge temperature of tank, the area of the high-temperature zone (red zone) has a large proportion. However, it would necessarily dissipate the heat to the environment, and that is why the temperature drop zones (blue or green zone) appear when the dimensionless time lengthens enough, whereas the ordinary tank has more of the blue area. In contrast, while dimensionless time is before 0.8, the outlet temperature in the PCMs tank is basically maintained at about 78 °C. As the inlet velocity declines, the outlet temperatures are inferior to the other flows. This is because the experiment takes longer at low velocity, and installation of insulation materials cannot prevent thermal exchange between the experimental apparatus and outside circumstances. Seen from Figure 6, when the water tank does not contain SAT, the outlet temperature of the water tank begins to drop after the dimensionless time of 0.6, and the inflection point temperature of the SAT tanks happens at 0.8–0.9. Compared with Figure 5, the PCM placed close to the water outlet helps to keep the water warm. As time goes by, the PCMs did not release a large quantity of heat and gradually did not have a reheating effect when passing through cold water. The volume of high-temperature water at the upper layer of the tank is small, the cold water rises rapidly, and the outlet water temperature drops rapidly. The maximum experimental standard error is 5.24, and the experimental data are reliable.

4.2. Filling Efficiencye

As Figure 7 presents, the FE in the phase change material tank and the common tank has a similar development trend over dimensionless time. While the inlet flow increased from 2 to 6 L/min, the FE increased, but while the inlet flow continued to increase, the FE decreased. When the flow rate was small, the municipal water did not submerge into the hot water violently, the water output of high-temperature water was relatively large, and the PCM storage ball fully released heat, thus increasing the FE. When cold water entered the tanks at lower flow, the FE in the operating condition containing PCMs became superior to the ordinary conditions. The case that had the flow rate arriving at 6 L/min had same the trend. As the flow rate was raised ulteriorly to 10 L/min, the impact for municipal water on the high-temperature water continued to increase. Simultaneously, the hot water was violently disturbed by the cold water, and the thickness of the thermocline increased, resulting in a decrease in FE. When the flow rate became 2 L/min, in the operating conditions containing PCMs and in the ordinary conditions, the FE values were 0.771 and 0.719, respectively. As the flow rate went up to 6 L/min, the filling efficiency was increased separately to 905 and 0.793. At the time that the inlet flow arrived at 10 L/min, the filling efficiency of the PCM storage tank dropped sharply to 0.593, which was greatly reduced, and the ordinary water tank was reduced to 0.769, which was less reduced. From the above descriptions, it could be inferred that the pure water had a higher specific heat capacity than the PCM balls under constant pressure, and it occupied a certain volume in the tank. Cold water which had an increasing velocity quickly replaced the hot water, and the PCM balls did not release enough latent heat. This prevented the PCMs balls from transferring a large amount of heat to the cold fluid immediately, which intensified the degree of municipal water soaking into the hot water, resulting in a decrease in the FE.

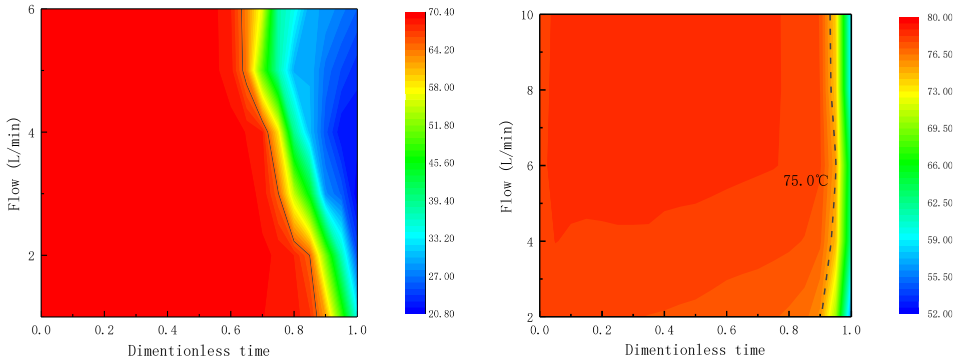

(**a**) No PCMs water tank (**b**) PCMs water tank

Figure 6. Temperature variations in the water tank outlet.

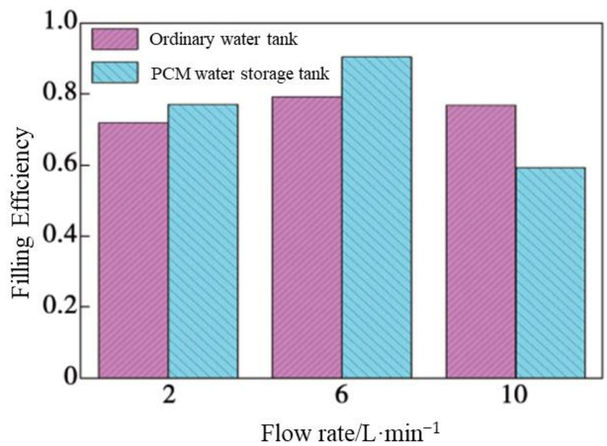

Figure 7. Fill efficiency variation curve.

4.3. MIX Number

Figure 8 displays the MIX variation curves under several flow rates. The change trend in the MIX value in the different water tanks during the exothermic process was similar. The mixing changes inside the water tank can be divided into three stages. As the dimensionless time came closer to 0.1, the MIX curves fell sharply. Then the slopes of the curves were gentle. Finally, the MIX went up rapidly again. By analyzing the curve trends, the PCMs storage tank and the common storage tank had a similar thermal stratification change. While the exothermic process began, immersion of low-temperature water disrupted the energy balance at the bottom of the water tank. Meanwhile, the high-density, low-temperature water dropped under gravity, while the high-temperature water floated upward under buoyancy, eventually causing thermal stratification. Therefore, the value of MIX decreased. With the increase in dimensionless time, the high-temperature water lost its energy and cooled down to the same temperature as the low-temperature water. That marked water temperature uniformity gradually became high. That also caused the thermal stratification to weaken, thus the MIX became larger.

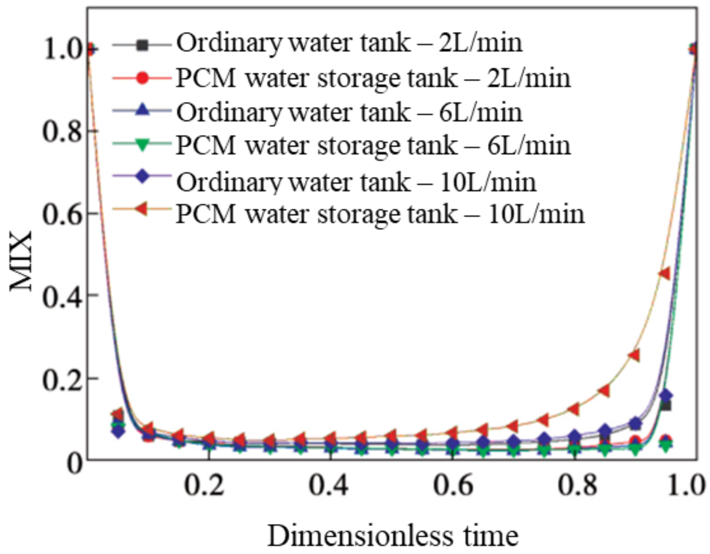

Figure 8. MIX number variation curve.

The PCM tank had a MIX value that was lower than the other tanks with an inlet flow of 6 L/min, and the performance of the stratification was better than that of the other tanks. The inhibition effect and heat exchange of PCMs weakened the interference of the low-temperature water in phase change material tank to hot water; it also increased the temperature of the cold water. In summary, the thermal stratification of water tanks with PCMs was improved. However, the high-temperature water in the tank was rapidly replaced as the flow rate increased; the phase change material balls did prevent the release of latent heat in time, resulting in a further increase in cold and hot water mixing. Therefore, the ordinary tanks had better thermal stratification than the tanks containing PCMs.

4.4. Exergy Efficiency

EE variation in respect to dimensionless time is shown in Figure 9. When the maximum flow was less than or equal to 6 L/min, the increase in the PCMs contributed to the EE variation. When the dimensionless time was zero, the EE in all of the tanks approximately equaled one. This indicated that the tank was filled with high-temperature water whose temperature was uniform at the beginning. The EE decreased gradually with the increase in dimensionless time after heat release. Under the flow condition of 6 L/min, the EE of the PCMs tank was 0.253 higher than the common tank, while the EE for the ordinary tank was only 0.373, at dimensionless time 0.95. The EE of the tank containing PCMs was always lower than that of the other water tanks during the exothermic process, while the flow rate was at 10 L/min. In addition, when the dimensionless time was between 0 and 0.95, the difference increased gradually, and when the dimensionless time was between 0.95 and 1, the difference decreased gradually.

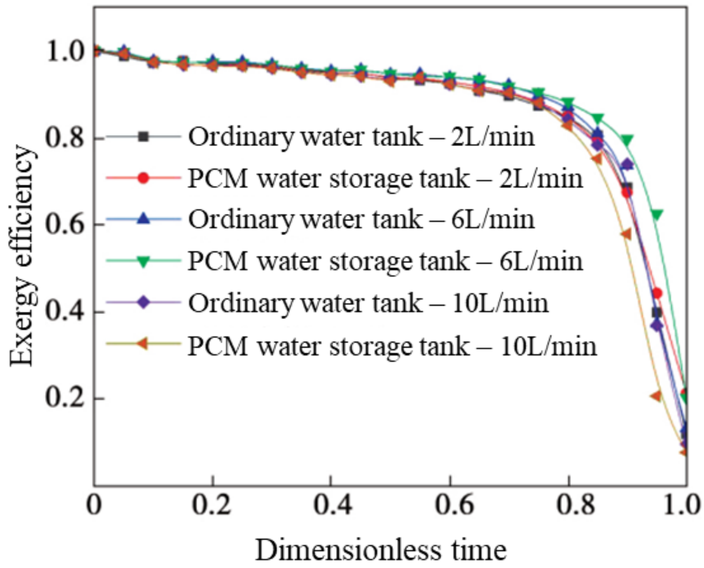

Figure 9. Exergy efficiency curves.

5. Conclusions

Multiple sets of experiments were conducted on a PCM test rig under the given working conditions. This article discusses the advantages of phase change materials from temperature, FE, EF, and MIX number. The following conclusions are drawn:

1. A new water inlet structure was designed, which reduces the water inlet speed, weakens the mutual immersion of high- and low-temperature water, and improves the heat stratification efficiency of the water storage tank. As the flow rates were less than or equal to 6 L/min, the PCMs provided additional heat to and reheat of the water temperature layer, which effectively ameliorated the stratification of the tanks. When the water flow increased to 10 L/min, the PCM balls were unable to release latent heat in time, and stratification effect was poor.
2. The filling efficiency as a new performance assessment criterion of tanks was defined. This value is colligated with the influence of the initial temperature of the storage tank, the intake temperature, the exit temperature, and the inlet flow on the performance. This is a relatively comprehensive measurement parameter. The FE of the tank containing PCM whose thermal stratification effect was better than the other tanks in the tests would reach 0.905 with a 6 L/min flow inlet.
3. The studied provided research of the influencing mechanisms of SAT heat storage followed by an emphasis on thermal stratification in tanks. The test results showed that the temperature change trend in each layer of the water tank was similar when the dimensionless time kept increasing. The higher the flow rate, the earlier the inflection points appears and the worse the stratification effect. In the meantime, the EE gradually decreased, and the FE increased first and then decreased. When the dimensionless time was 0.95, its EE was about 1.404 times that of the ordinary tank with the same flow rate.

Author Contributions: Conceptualization, H.Z.; investigation, F.X.; writing—original draft preparation, J.H.; writing—review and editing, Z.W. All authors have read and agreed to the published version of the manuscript.

Funding: This work was supported by the Shanghai Municipal Natural Science Foundation (20ZR1438600), the Special Project of Biomedical Science and Technology Support of Shanghai Science and Technology Innovation Action Plan (21S31900200), the Open Project of the Shanghai Key Laboratory of Multiphase Flow and Heat Transfer in Power Engineering and the Central Guidance on Local Science and Technology Development Fund of Shanghai City (YDZX20213100003002), and the Special Project of Independent Innovation of Qingdao City (21126NSH).

Data Availability Statement: Not applicable.

Conflicts of Interest: The authors declare no conflict of interest.

Nomenclature

τ	Dimensionless time
t	Water inlet time of the tank(s)
θ	Time to completely replace the whole box of water at the current flow
Q_{w}	Energy of ordinary hot water storage tank (J)
C_{P}	Constant pressure specific heat capacity of the water (J/(kg·K))
ρ_{w}	Density of the water (kg/m)
V_{T}	Volume of the water tank (m)
T_{hot}	Temperature of the hot water (K)
T_{cold}	Temperature of the cold water (K)
Q_{PCM}	Energy of the PCM water tank (J)
V_{P}	Volume of the PCM storage ball (m^3)
ρ_{PCM}	Density of the PCM storage ball (kg /m^3)
C_{pl}	Liquid specific heat capacity of the PCM (J/(kg·K))
T_{l}	Liquid temperature of PCM (K)
L	Latent heat of the PCM (J/kg)
C_{ps}	Solid specific heat capacity of the PCM (J/(kg·K))
T_{s}	Solid state temperature of the PCM (K)
MIX	MIX number
M_{e}	Momentum of the experimental water tank (J·m)
M_{s}	Momentum of the perfectly stratified tank (J·m)
V_i	Volume of water tank layer i (m^3)
y_i	Vertical distance from the center of gravity of the first floor of the tank to the bottom of the tank (m)
E_i	Energy of layer i of the water tank (J)
E_{e}	Energy of the experimental water tank (J)
E_{s}	Energy of the perfectly stratified water tank (J)
V_{h}	Perfectly stratified tank's hot water volume (m^3)
V_{c}	Perfectly stratified tank's cold water volume (m^3)
D	Diameter of the water tank (m)
H	Height of the water tank (m)
y_{s}	Vertical distance from the thermocline center to the tank bottom (m)
$E_{\mathrm{s},i}$	Energy of layer I of the perfectly stratified water tank (J)
m_i	Quality of water tank layer I (kg)
T_i	Temperature of water tank layer I (K)
T_{e}	Water tank outlet temperature (K)
T_{in}	Water tank inlet temperature (K)
ξ_{e}	Exergy value of the experimental water tank (J)
ξ_{s}	Exergy value of the perfectly stratified water tank (J)

References

1. Mao, Q.J.; Liu, N.; Peng, L. Preparation and characterization of a novel composite phase change heat storage material. *Renew. Energy* **2018**, *36*, 1574–1580.
2. Kurşun, B. Effect of rectangular hot water tank position and aspect ratio on thermal stratification enhancement. *Renew. Energy* **2018**, *16*, 639–646. [CrossRef]
3. Zhang, H.T.; Zhao, Y.J.; Zhang, P.; Shi, L.J.; Li, J.L. Research progress of heat storage materials of molten nitrate in solar energy utilization. *Mater. Rev.* **2015**, *29*, 54–60.
4. Zhu, M.S.; Wang, Z.L.; Zhang, H.; Sun, X.X. Experimental investigation of the comprehensive heat transfer performance of PCMs filled with CMF in a heat storage device. *Int. J. Heat Mass Transf.* **2022**, *188*, 122582. [CrossRef]
5. Wang, Z.L.; Zhang, H.; Dou, B.L.; Wu, W.D. Effect of copper metal foam proportion on heat transfer enhancement in the melting process of phase change materials. *Appl. Therm. Eng.* **2022**, *201*, 117778. [CrossRef]
6. Turski, M.; Jachura, A. Life cycle assessment of dispersed phase change material heat accumulators for cooperation with buildings in the district heating system. *Energies* **2022**, *15*, 5771. [CrossRef]
7. Hua, W.S.; Zhang, X.L.; Ding, J.H.; Liu, F. Design and research of compound heat storage tank. *Build. Energy Effic.* **2016**, *44*, 108–113.

8. Zhou, Y.K.; Yu, Z.; He, J.A. Model and Application of a Domestic Hot-Water Tank with a Novel Structure Comprising a Phase-Change Material. *Build. Sci.* **2017**, *33*, 27–33.
9. Brumleve, T.D. *Sensible Heat Storage in Liquids*; Report No. SLL-73-0263; Sandia National Laboratories: Albuquerque, NM, USA, 1974.
10. Frazzica, A.; Manzan, M.; Sapienza, A. Experimental testing of a hybrid sensible-latent heat storage system for domestic hot water applications. *Appl. Energy* **2016**, *18*, 1157–1167. [CrossRef]
11. Ramana, A.S.; Venkatesh, R.; Antony, A.R.V. Experimental investigation of the LHS system and comparison of the stratification performance with the SHS system using CFD simulation. *Sol. Energy* **2014**, *103*, 378–389. [CrossRef]
12. Bellan, S.; Alam, T.E.; Gonzalez-Aguilar, J. Numerical and experimental studies on heat transfer characteristics of thermal energy storage system packed with molten salt PCM capsules. *Appl. Therm. Eng.* **2015**, *90*, 970–979. [CrossRef]
13. Kumar, G.S.; Nagarajan, D.; Chidambaram, L.A. Role of PCM addition on stratification behaviour in a thermal storage tank—An experimental study. *Energy* **2016**, *15*, 1168–1178. [CrossRef]
14. Panchabikesan, K.; Antony Aroul Raj, V.; Ding, Y. Enhancement in free cooling potential through PCM based storage system integrated with Direct Evaporative Cooling (DEC) unit. *Energy* **2017**, *144*, 443–455. [CrossRef]
15. Koca, A.; Oztop, H.F.; Koyun, T. Energy and exergy analysis of a latent heat storage system with phase change material for a solar collector. *Renewable Energy* **2008**, *33*, 567–574. [CrossRef]
16. Bony, J.; Citherlet, S. Numerical model and experimental validation of heat storage with phase change materials. *Energy Build.* **2007**, *39*, 1065–1072. [CrossRef]
17. Abdelsalam, M.Y.; Sarafraz, P.; Cotton, J.S. Heat transfer characteristics of a hybrid thermal energy storage tank with Phase Change Materials (PCMs) during indirect charging using isothermal coil heat exchanger. *Solar Energy* **2017**, *157*, 462–476. [CrossRef]
18. Navarro, L.; Barreneche, C.; Castell, A. High density polyethylene spheres with PCM for domestic hot water applications: Water tank and laboratory scale study. *J. Energy Storage* **2017**, *13*, 262–267. [CrossRef]
19. Prieto, M.M.; González, B.; Granado, E. Thermal performance of a heating system working with a PCM plate heat exchanger and comparison with a water tank. *Energy Build.* **2016**, *122*, 89–97. [CrossRef]
20. Najafian, A.; Haghighat, F.; Moreau, A. Integration of PCM in domestic hot water tanks: Optimization for shifting peak demand. *Energy Build.* **2015**, *5*, 55–64. [CrossRef]
21. Deng, J.; Furbo, S.; Kong, W. Thermal performance assessment and improvement of a solar domestic hot water tank with PCM in the mantle. *Energy Build.* **2018**, *172*, 10–21. [CrossRef]
22. Kicsiny, R. Black-box model for solar storage tanks based on multiple linear regression. *Renew. Energy* **2018**, *125*, 857–865. [CrossRef]
23. Afshan, M.E.; Selvakumar, A.S.; Velraj, R.; Rajaraman, R. Effect of aspect ratio and dispersed PCM balls on the charging performance of a latent heat thermal storage unit for solar thermal applications. *Renew. Energy* **2019**, *148*, 876–888. [CrossRef]
24. Cabeza, L.F.; Ibanez, M.; Sole, C. Experimentation with a water tank including a PCM module. *Sol. Energy Mater. Sol. Cells* **2006**, *9*, 1273–1282. [CrossRef]
25. Zalba, B.; Marín, J.M.; Cabeza, L.F. Review on thermal energy storage with phase change: Materials, heat transfer analysis and applications. *Appl. Therm. Eng.* **2003**, *23*, 251–283. [CrossRef]
26. Sharma, S.D.; Sagara, K. Latent heat storage materials and systems: A review. *Int. J. Green Energy* **2005**, *2*, 51–56. [CrossRef]
27. Ibáñez, M.; Cabeza, L.F.; Solè, C. Modelization of a water tank including a PCM module. *Appl. Therm. Eng.* **2006**, *26*, 1328–1333. [CrossRef]
28. Berkel, J.V. Mixing in thermally stratified energy stores. *Solar Energy* **1996**, *58*, 203–211. [CrossRef]
29. Ievers, S.; Lin, W. Numerical simulation of three-dimensional flow dynamics in a hot water storage tank. *Appl. Energy* **2009**, *86*, 2604–2614. [CrossRef]
30. Altuntop, N.; Arslan, M.; Ozceyhan, V. Effect of obstacles on thermal stratification in hot water storage tanks. *Appl. Therm. Eng.* **2005**, *25*, 2285–2298. [CrossRef]
31. Allouche, Y.; Varga, S.; Bouden, C. Validation of a CFD model for the simulation of heat transfer in a tubes-in-tank PCM storage unit. *Renew. Energy* **2016**, *89*, 371–379. [CrossRef]
32. Wang, Z.L.; Zhang, H.; Dou, B.L.; Huang, H.J.; Wu, W.D.; Wang, Z.Y. Experimental and numerical research of thermal stratification with a novel inlet in a dynamic hot water storage tank. *Renew. Energy* **2017**, *111*, 353–371. [CrossRef]
33. Davidson, J.H.; Adams, D.A. Fabric stratification manifolds for solar water heating. *J. Sol. Energy Eng.* **1994**, *3*, 130–136. [CrossRef]
34. Njoku, H.O.; Ekechukwu, O.V.; Onyegegbu, S.O. Analysis of stratified thermal storage systems: An overview. *Heat Mass Transf.* **2014**, *50*, 1017–1030. [CrossRef]